-RESEARCH PAPER-

International Journal of Mining and Geo-Engineering

IJMGE

IJMGE 57-4 (2023) 381-387

DOI: 10.22059/IJMGE.2023.355306.595036

A multi-disciplinary and exploratory geospatial data set integration for porphyry copper prospectivity mapping in Kerman belt, Iran

Sareh Sadigh [a], Mirsaleh Mirmohammadi [a,*], Alok Porwal [b]

[a] *School of Mining Engineering, College of Engineering, University of Tehran, Tehran.*

[b] *Centre for Studies in Resources Engineering, Indian Institute of Technology Bombay, India.*

Article History:

Received: 13 February2023.

Revised: 19 May 2023.

Accepted: 22 May 2023.

ABSTRACT

The Mineral Prospectivity Map (MPM) is a powerful tool for identifying target areas for the exploration of undiscovered mineral deposits. In this study, a knowledge-driven Index overlay technique was utilized to create the MPM on a regional scale. The complex distribution patterns of geological features associated with mineral deposits were mapped and correlations between these features and mineral deposits were revealed by integrating geological, geophysical, hydrothermal alteration, and fault density data layers. It was found that 23% of the study area was highly prospective, with 77% of the known porphyry copper occurrences located within this area. The normalized density was equal to 3.35, indicating a significant relationship between the known porphyry copper occurrences and their occupied area. The MPM also identified potential tracts outside the known mineralized areas that can be used for exploration and quantitative assessment of undiscovered resources. It is suggested that the MPM is a valuable tool for mineral exploration and could have significant implications for the mining industry.

Keywords: *Index overlay, Kerman Cenozoic Magmatic Belt, mineral prospectivity map, porphyry copper deposit, prediction-area (P-A) plot.*

1. Introduction

The Mineral Prospectivity Map (MPM) is a multi-criteria decision-making task aimed at identifying target areas for exploring undiscovered mineral deposits of a specific type [1], [2]. This task is challenging because mineral deposits result from complex interactions of deposit-forming processes that manifest in various geological features. These features lead to nonlinear correlations between mineral occurrences and geological characteristics, making them difficult to analyze using traditional approaches primarily based on empirical judgment [3].

In the field of integration, significant studies have been conducted on regional and local scales within the Kerman belt. Abedi et al. examined the performance of the ELECTRE III multi-criteria knowledge-driven decision-making method in creating a mineral potential map for the Nouchun mine in the Kerman belt [4], [5]. They also proposed a knowledge-based method using witness belief functions and applied the Dempster-Shafer combination law to create a mineral potential map for the Saridune deposit. Additionally, they explored other methods such as index overlay techniques and fuzzy logic, comparing them with the introduced method [6].

Shabankareh and Hezarkhani introduced the support vector classification method to integrate exploration data on a regional scale for creating a copper prospecting map in the Kerman copper belt [7]. Ghasemzadeh et al. evaluated and compared U-statistics and fractal models to identify geochemical anomalies and their distribution patterns in the Baft area, located within the Kerman belt. They introduced a mineral prospecting model by integrating the geochemical layer and the geological layer on a regional scale to target exploration in the study area [8].

Rahimi et al. conducted a study analyzing the impact of utilizing different numbers of non-deposit locations compared to a consistent number of well-known deposit locations on the effectiveness of exploration targeting models. This study centered on the Chahargonbad geological map in the Kerman belt [9]. Bonham-Carter (1994) introduced the Index Overlay method for knowledge-driven MPM, in which both the weights of evidential maps and the values of classes in each evidential map are determined by expert opinions and weighted accordingly [10].

The main aim of this paper is to identify the best target areas by combining four evidential data layers: the geological map, geophysical map, structural map, and hydrothermal alteration map, using the Index Overlay method. During this process, weights are assigned to each evidential map based on expert opinions, and the resulting weighted map is utilized as an input for integration. Additionally, the weight of the Modified Predictive Map (MPM) is determined through the prediction-area (P-A) plot. As a result, the study area is narrowed down, reducing the risk associated with exploration operations. By following these detailed steps, permissive areas can be identified with greater certainty, allowing focused exploration efforts to be directed toward them.

2. Study Area: The Kerman Belt

The Kerman Cenozoic Magmatic Arc (KCMA), also known as the Kerman Belt, is situated in the southeastern part of the Urumieh-Dokhtar Magmatic Belt (UDMB). It is widely regarded as the most promising geological province for porphyry copper deposits in Iran, as depicted in Figure 1 (Aghazadeh et al., 2015). Porphyry copper

* Corresponding author. *E-mail address:* m.mirmohammadi@ut.ac.ir (M. Mirmohammadi).

mineralization occurs within Oligocene-Miocene intrusive bodies within the UDMB. The Kerman Belt, spanning 40 to 50 km in width, follows a northwest-southeast trend within the UDMB, stretching for a length of 400 km and bordered by significant strike-slip faults. The northern margin of the Kerman Belt is delineated by the Rafsanjan and Sarvestan faults, while its southern margin is defined by the Nain-Baft and Sarbizan faults. The emplacement of porphyry and porphyry copper deposits in the UDMB can be attributed to Tertiary-related tectonic processes and the closure of the Neo-Tethys Ocean, as observed in previous studies (Agard et al., 2005; McInnes et al., 2005; Richards et al., 2012; Shafiei et al., 2009).

The Kerman Belt can be characterized by two primary phases of intrusions: an Eocene-Oligocene phase known as "Jebal Barez" and a mid-late Miocene dioritic to granodioritic phase called "Kuh Panj." Jebal Barez is situated in the southeast and center of KCMA and is composed of composite gabbroic to granitic intrusive rocks and their volcanic counterparts. Meanwhile, Kuh Panj, located in the northwest and center of KCMA, consists of porphyritic-textured granodioritic intrusive rocks and Miocene dioritic formations (Shafiei et al., 2009).

The Kuh Panj region harbors a significant number of porphyry copper deposits, whereas the deposits in Jebal Barez are limited in number (Aghazadeh et al., 2015).

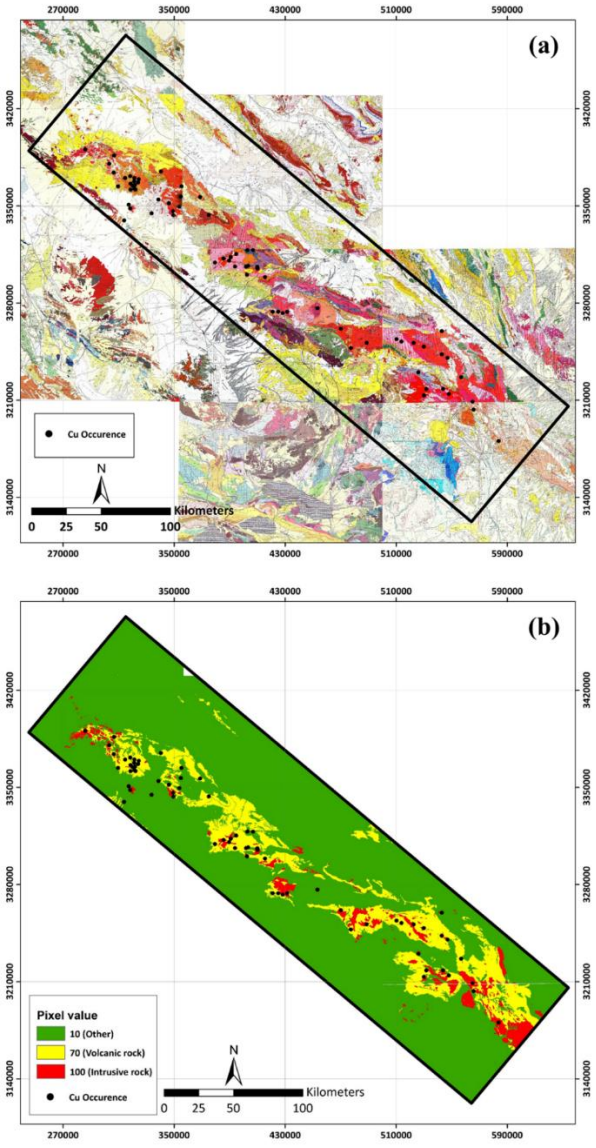

Figure 1. (a) discrete geological map (b) discrete map of weighted rock units.

3. Data and Methods

3.1. Data

3.1.1. Porphyry copper deposits

The study utilized mineral deposit data primarily compiled from the exploratory report by the United States Geological Survey (USGS) [11]. The locations of major deposits were further reviewed and refined by considering satellite-based images and internal reports from the National Iranian Copper Industries Company. All mineral deposits were represented as point features with the coordinates of their centroids. The study included a total of 70 deposit points, consisting of 17 mines and 53 occurrences/prospects.

3.1.2. Evidence data layers

Based on the conceptual model of prospectivity for porphyry copper deposits and the available data, this study employed four evidence layers to generate a mineral prospectivity map (MPM). These evidence layers include the geological map, geophysical map, structural map, and hydrothermal alteration map. The selection of these layers was guided by the conceptual model of porphyry copper deposit prospectivity.

To generate the MPM, the spatial evidence values of the four maps were transformed into a range of [0, 1] using a logistic function. It is important to mention that the cell dimension for all maps utilized in this study was set to 30 m x 30 m.

By integrating the evidence layers and applying the transformation, the resulting MPM offers a comprehensive perspective on areas that potentially harbor porphyry copper deposits. The incorporation of multiple evidence layers overcomes limitations tied to individual data sources and ensures a more precise depiction of prospectivity.

The integration of these evidence layers and the transformation method employed in this study establishes a reliable framework for pinpointing potential areas for porphyry copper deposits. The resultant MPM proves to be a valuable instrument for mineral exploration and resource assessment in the study area.

Geological map

Geological maps serve as essential tools for identifying permissive tracts for various types of deposits. Descriptive models of these deposits help in pinpointing the tectonic structures and geological environments contributing to each type. Accurate recognition of geological structures associated with specific deposits requires the use of high-resolution geological maps and expert knowledge. Ideally, the most appropriate map for identifying permissive tracts should align with the scale of the final evaluation map. In this context, the primary purpose of the evidence layer is to extract geological units linked to porphyry copper deposits.

To achieve this goal, the study utilized geological maps at a scale of 1:250,000 generated by the Geological Survey and Mineral Exploration of Iran. These maps played a crucial role in identifying rock units associated with porphyry copper deposits. Specifically, eight maps were examined, namely Yazd, Anar, Rafsanjan, Neyriz, Sirjan, Bam, Hajiabad, and Sabzevaran. The boundaries of these maps were assimilated, and their corresponding rock units were integrated to establish a comprehensive understanding of the region's geology.

The next step in this investigation involved simplifying the maps and dividing the geological formations into three units: Miocene-Oligocene intrusive bodies related to porphyry copper mineralization in the Kerman belt, volcanic rock, and other units. The resulting information can be used to identify areas that are potentially permissive for porphyry copper deposits.

It is worth noting that correctly identifying geological structures associated with different types of deposits requires a high-resolution geological map and specialized knowledge. Therefore, it is crucial to use the most appropriate map corresponding to the scale of the final evaluation map. Descriptive models of deposits are also critical in identifying tectonic structures and geological environments associated

with each type of deposit. In essence, geological maps serve as a fundamental source of information for identifying and determining permissive tracts for various types of deposits.

Geophysical map

Geophysical methods are essential for identifying and delineating potential mineral deposit targets. While direct detection of targets may be possible in small study areas or where alteration zones are clearly evident, this is not typically the case for exploration at larger scales. Geophysical surveys, such as airborne magnetics, are often used to identify hidden permissive rock units covered by younger sediments, thus providing crucial information on the primary boundaries of exploration areas.

Geological maps serve as the primary source of information for delineating target areas but often lack details on overlying rock units, making geophysics a valuable tool for determining the lateral and vertical extent of geological units. Geophysical mapping can also assist in identifying permissive geologic environments for specific mineral deposits, including crustal structures, major margins, plutons, and hidden calderas. Additionally, geophysical maps provide crucial information on magnetic rocks associated with certain mineral deposits.

In this paper, airborne magnetic data (reduced to pole) is utilized to investigate the magnetic anomalies of a region as an input layer for the integration process (Figure 2). It is worth noting that geophysical maps not only assist in identifying anomalies and shallow bodies but also differentiate regional structures and lineaments, thereby significantly contributing to the understanding of the geologic context of mineral deposits.

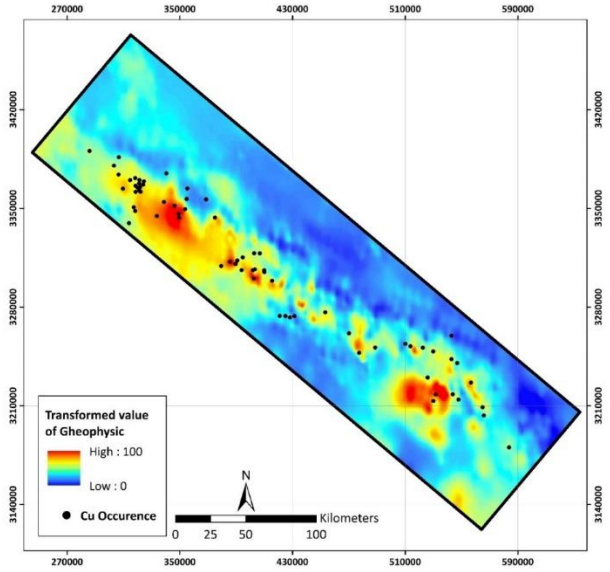

Figure 2. Map of geophysical anomalies with normalized continuous value

Hydrothermal alteration map

Porphyry copper deposits are commonly associated with hydrothermal alteration zoning that includes potassic, phyllic, and propylitic alteration from the center outward [12]. The presence and extent of alteration are often indicators of the scale and intensity of ore enrichment. It is well-established that the ore body is typically located in the quartz-phyllic or potassic alteration zone, with larger deposits exhibiting stronger alteration and richer mineralization [12], [13]. In this study, the ASTER sensor data and the spectral angle mapper (SAM) method were used to identify hydrothermal alteration minerals and highlight alteration zones (Figure 3). The SAM method is a rapid classification technique that compares the spectral similarity between the image spectrum and a reference reflectance spectrum [14].

The similarity is calculated based on the angle between two spectra, which are represented as vectors in an n-dimensional space, where n is the number of spectral bands. The reference spectrum can be obtained from field and laboratory measurements or directly from satellite images. The SAM method calculates the spectral similarity by computing the angle between two spectra, with a small angle indicating high similarity and a large angle indicating low similarity. The angle measurement ranges from zero to one [15].

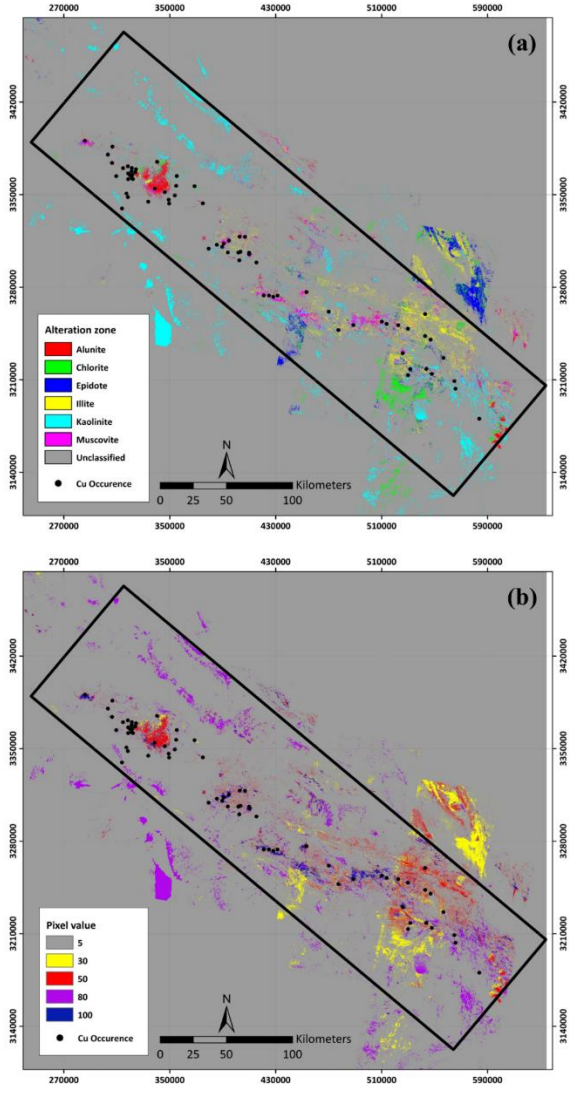

Figure 3. (a) discrete map of hydrothermal alteration and (b) discrete map of weighted hydrothermal alteration.

Fault and structures map

The correlation between faulting, fluid flow, and deposit formation processes is well-established [16]–[18]. Structural analysis conducted on primary copper deposit belts worldwide indicates that the positioning of intrusive masses and associated copper deposits is influenced by the transpression process [19]–[21]. In this specific tectonic context, dextral strike-slip faults create suitable structural basins, such as duplex faults, for the placement of porphyry copper deposits. To identify linear structures, this study uses two layers of information. The first layer involves identifying faults depicted on the geological map at a scale of 1:250,000. The second layer involves applying reduction-to-pole and

analytic signal filters to airborne geophysical data to identify potential linear structures concealed at greater depths below the Earth's surface (figure 4).

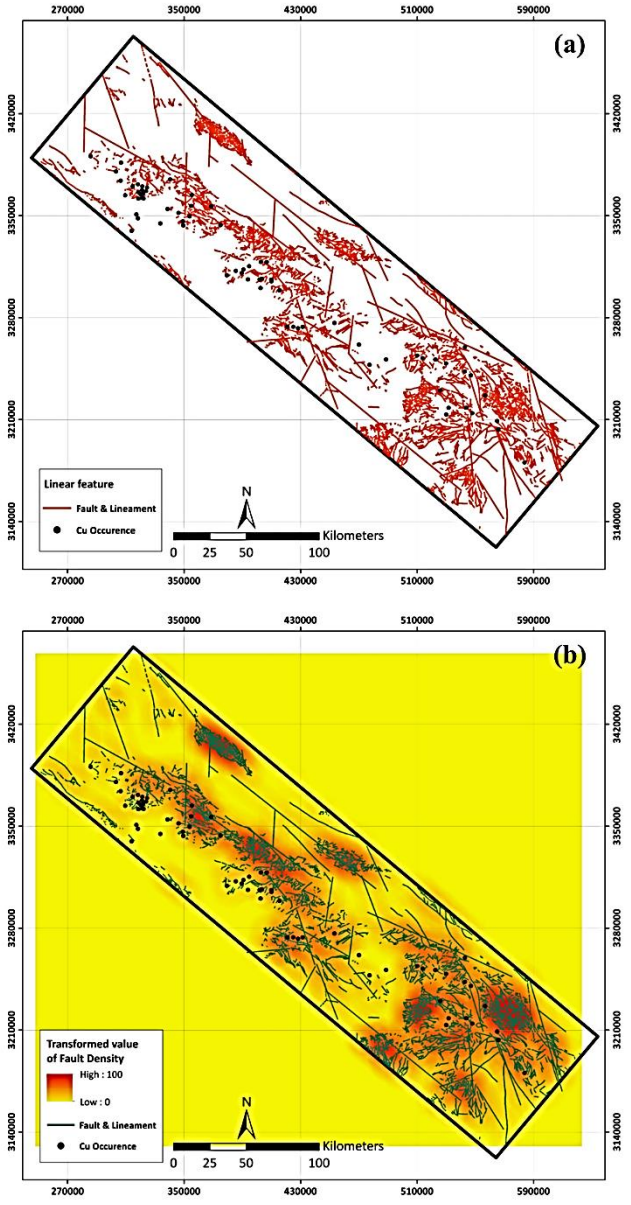

Figure 4. (a) fault density map and (b) normalized continuous fault density map.

3.2. Methods

Multi-class index overlay

Multi-class index overlay is a method utilized to create knowledge-based mineral potential maps. This method involves discretizing evidence maps into arbitrary classes and integrating them by assigning subjective weights to each evidence map. A score S_{ij} is assigned to each of the j^{th} classes from the i^{th} evidence map according to their relative importance. The relative importance of an evidence map compared to any other evidence map is controlled by the assigned weights W_i. The weighted evidence maps are then combined using the following equation, calculating a ($\overline{IO}$) score for each pixel [10]:

$$IO = \frac{\sum_i^n S_{ij} W_i}{\sum_i^n W_i} \quad (1)$$

Which for the present study is defined as:

$$IO = \frac{S_{geo}W_{geo}+S_{gph}W_{gph}+S_{rs}W_{rs}+S_{fd}W_{fd}}{W_{geo}+W_{gph}+W_{rs}+W_{fd}} \quad (2)$$

Where W_{geo}, W_{gph}, W_{rs} and W_{fd} are respectively the weights of geological, geophysical, remote sensing (hydrothermal alteration) and fault density maps, which are determined based on expert opinion. Also, S_{geo}, S_{gph}, S_{rs}, and S_{fd} are the transformed values of each pixel, which are determined in layers with continuous values by logistic functions and in discrete layers by experts.

4. Result

4.1. Integration of evidence map

In the context of Mineral Potential Mapping (MPM), weighted evidence maps are combined through mathematical fusion functions that delineate the relative importance of each evidence map [10], [22]–[25]. In this study, evidence maps were transformed into the [0,1] range utilizing a logistic function [26], [27], and the weights of the evidence maps were determined through a knowledge-driven method involving expert opinions. To identify target areas, mathematical fusion functions were applied, taking into account both sets of weights mentioned earlier. Specifically, the index overlay model proposed by Bonham-Carter was utilized to integrate the evidence layers [10].

In this research, two different types of data layers are dealt with. The first category comprises evidence maps with continuous quantitative values, and the second category consists of maps with discrete qualitative values. Geophysical and fault density layers are continuous, whereas geological and alteration layers contain qualitative information, requiring the assignment of numeric values to each pixel. Based on the significance of rock units in the geological map and the indicator minerals resulting from alteration in porphyry copper deposits, each of these layers is classified, and the classes are valued based on their relative importance using a knowledge-based method (see Table 1).

In contrast to the geological and alteration maps, the geophysical and fault density maps contained continuous quantitative values ranging from 0 to 1, and did not require a knowledge-based method for assigning values to each pixel.

It is essential to note that in this study, the weights of the evidence maps were determined using a knowledge-driven method reliant on expert opinions (refer to Table 2).

Table 1. Valuation of qualitative data layers by knowledge-driven methods.

Data layer	Class	Value (Weight)
Geology map	Intrusive rock (Miocene- Oligocene)	1
	Volcanic rock	0.7
	Other	0.1
Alteration map	Muscovite	1
	Kaolinite	0.8
	Illite	0.5
	Alunite	0.5
	Chlorite and Epidote	0.3

Table 2. Relative valuation of evidence maps by knowledge-driven method.

Evidence map	Weight
Geology map	0.95
Alteration map	0.93
Geophysic map	0.9
Fault density map	0.5

After preprocessing each evidence layer, the input data layers underwent processing to generate the mineral prospectivity map of porphyry deposits within the metallogenic belt of Kerman, as depicted in Figure 5. Because all the evidence maps consist of pixel values ranging from 0 to 1, the resulting mineral prospectivity map is also a continuous

map with pixel values within the same range. It is apparent that pixels with higher values or scores (approaching 1) hold greater significance and are more likely to encompass porphyry copper deposits.

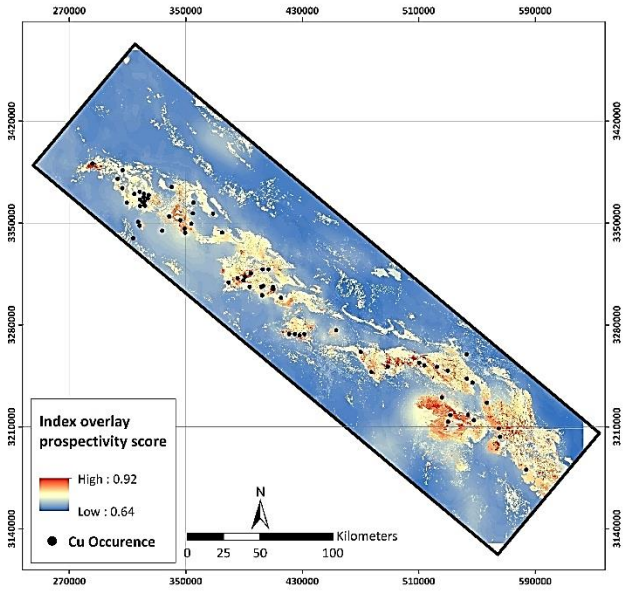

Figure 5. The map of index overlay potential scores produced by combining the discrete map of weighted rock units, the continuous map of normalized geophysical anomalies, the discrete map of weighted hydrothermal alteration and normalized continuous fault density map.

4.2. Evaluation of the prospectivity map

The most effective method for evaluating the validity and accuracy of the generated model and its target areas is through field observations. Nevertheless, the model's accuracy can also be confirmed by considering the locations of known porphyry copper deposits. In particular, the correlation between established mineral deposits and various categories within the prospectivity map can be analyzed by superimposing deposit locations onto a discrete model [23]–[26], [28]. This assessment can be conducted using a prediction-area (P-A) plot. By comparing the MPM weight with the weight of the evidence layers, the integration map can be validated.

4.3. Prediction-area (P-A) plot

Mihalasky and Bonham-Carter employed a normalized density approach to assign weights to layers. Normalized density is calculated by dividing the prediction rate of each class by the corresponding occupied area relative to the entire studied area. The intersection point in the P-A diagram is utilized to determine the parameters required for calculating normalized density. Hence, the formula for calculating normalized density for weighting MPM is as follows [30]:

$$N_d = \frac{P_r}{O_a}$$

Where N_d is the normalized density, P_r and O_a are the prediction rate and the included area, respectively. These values are derived from the intersection point of the two curves in the P-A plot. Consequently, the weight assigned to the layer is:

$$W_E = Ln\, N_d$$

The fractal method (C-A) has been used to discretize and determine the class in the MPM Figure 6.

The intersection point on the P-A plot holds significance in evaluating the validity of the MPM model. In this instance, the intersection point reveals that the MPM model predicts 23% of the study area as having high potential, with 77% of the established porphyry copper occurrences situated within this region (refer to Fig. 7). This implies that the normalized density, calculated as the prediction rate of each class divided by the corresponding occupied area in relation to the entire study area, equals 3.35 (77/23). A normalized density surpassing 1 signifies a strong predictive capacity for potential mineral areas. Consequently, the MPM map bears a weight of 1.21 (Ln 3.35), signifying a substantial correlation between the known porphyry copper occurrences and their spatial extent. This outcome corroborates the validity and precision of the MPM model, indicating that the zones identified by the index overlay prospectivity map can serve as promising targets for further exploration efforts.

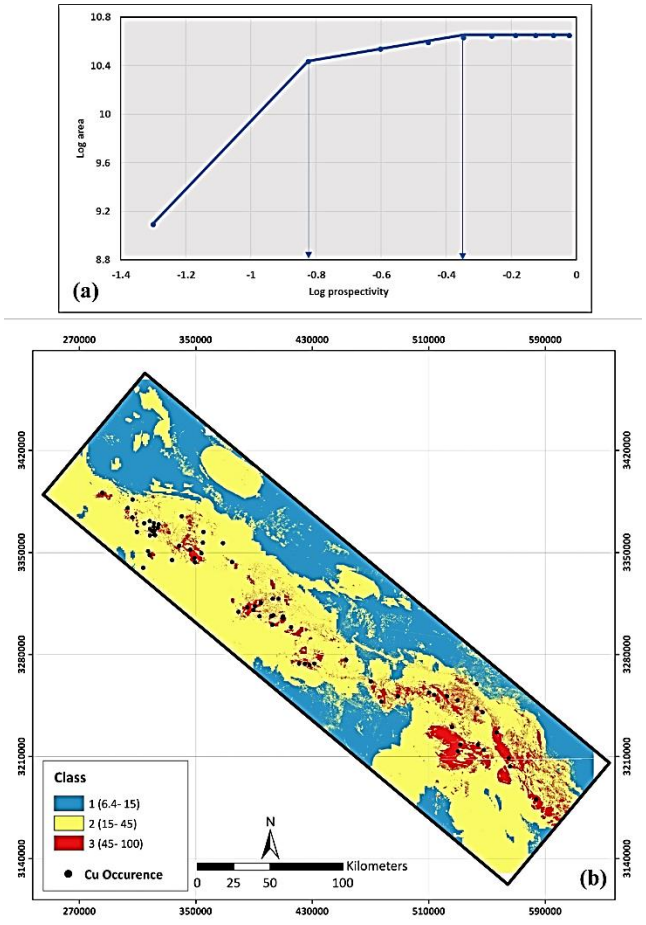

Figure 6. (a) (C-A) plot for multi-index overlay prospectivity values and (b) discrete index overlay prospectivity map.

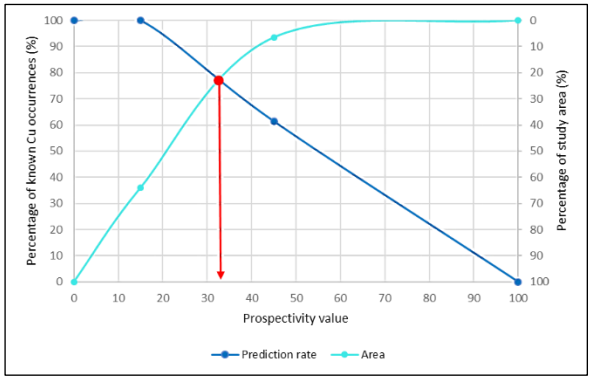

Figure 7. Prediction-area (P-A) plot for the discrete index overlay prospectivity map.

Additionally, the intersection point of the two curves on the horizontal axis of the P-A plot provides a threshold value for distinguishing areas with high-potential probability from those with lower potential. Thus, as depicted in Figure 8, any pixel with a value above 33 is considered a potential target area for further exploration.

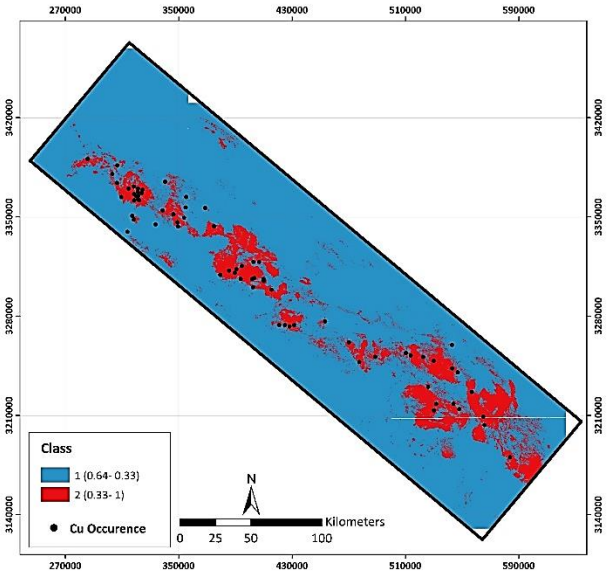

Figure 8. The target areas determined by the P-A plot.

5. Discussion

Porphyry copper deposits are typically discovered through surface outcrops and evidence. However, without a thorough understanding of subsurface processes, identifying covered target areas becomes impossible. The index overlay model adopts a knowledge-driven approach, assigning weights to evidence layers based on their relative importance and effectiveness in the formation process of porphyry copper deposits.

Through the use of a data-driven method and the P-A plot, the determination of the weight for the mineral prospectivity map and the evaluation of the prospectivity model have been achieved. The weight of evidence maps for the geological map, alteration map, geophysical map, and fault density map are 0.95, 0.93, 0.90, and 0.5, respectively. Meanwhile, the weight of the integrated map is 1.21 (normalized density 3.35). According to the theory of Mihalasky and Bonham-Carter, evidence layers and prospectivity models with a normalized density higher than 1 are considered suitable predictors.

The prospectivity map generated has been compared with previous exploration activities and the locations of known deposits. The Mineral Prospectivity Map (MPM) has predicted approximately 77% of the known occurrences and has also identified potential tracts beyond the known mineralized areas. These areas can be used for exploration and quantitative assessment of undiscovered resources.

The integration of data-driven and knowledge-driven approaches can yield more reliable results, depending on the type of data and the depth of understanding in the case study. Some areas identified as target zones in the prospectivity map of the Kerman belt might lack discovered deposits due to limited exploration efforts or complete lack thereof. These areas are the focus of this research, where a potential map is being prepared. Many surface deposits show no clear signs of mineralization because the intrusive bodies associated with mineralization are located beneath the surface or are covered by young sediments. While a geological map is essential for preparing a prospectivity map, it is not sufficient. Therefore, the incorporation of data layers, such as geophysical anomalies, including subsurface information, is strongly required.

In contrast to the other evidence layer, the weight of fault density suggests that a robust correlation between the location of porphyry copper deposits and fault density in the study area does not exist. This finding may imply a limited hydrological connection to the extensive vertical pathways for fluids originating from the lower crust. Consequently, it is recommended to utilize a novel geological point feature, specifically the intersection of faults and intrusive bodies, to effectively map the upward flow of fluids [31].

The target areas containing a higher number of porphyry copper occurrences are predominantly situated in the northwestern part of the Kerman belt (Sarduieh–Dahaj sector), whereas areas with fewer porphyry copper occurrences are mainly found in the southeastern part of the Kerman belt (Jebal-e-Barez sector). As illustrated in Fig. 8, the Jebal-e-Barez sector exhibits airborne geophysical anomalies, yet a significant number of discovered deposits in this sector remain unlocated. This phenomenon could be attributed to the presence of Oligocene granitoids' intrusive bodies at greater depths in the southeastern sector of the Kerman belt. These bodies are concealed by the Jebal-e-Barez mountain range in most areas and remain largely unexplored geologically [32], [33].

The limited number of discovered deposits in the southeastern part of Kerman does not necessarily indicate barren intrusive bodies in this sector; rather, it could be a consequence of insufficient exploration. The target areas in the northwest of the Kerman belt (Sarduieh–Dahaj sector) are comparatively smaller than their counterparts in the southeast (Jebal-e-Barez sector). Consistent with earlier geological studies by Dimitrijevic and Djokovic, the southern part of the Kerman belt comprises large granitoid bodies [34]. These bodies are situated deeper beneath the surface in comparison to the shallow granodiorite porphyries found in the northern part of Kerman.

6. Conclusions

This study aimed to recognize and analyze the favorable areas for further porphyry copper exploration in the Kerman Belt using the Index Overlay integration method. Based on the results of these analyses, the following conclusions were drawn.

(1) Integrating data-driven and knowledge-driven approaches can lead to more reliable results, depending on the type of data and the level of knowledge of the specific case study.

(2) The index overlay prospectivity map indicates that 23% of the study area has potential, with 77% of known porphyry copper occurrences located within this area.

(3) The granitoid bodies in the southern part of the Kerman belt are located at greater depths compared to the shallow granodiorite porphyries found in the northern part of Kerman.

(4) The MPM demonstrates high efficiency in identifying potential tracts outside of known mineralized areas, making it a valuable tool for exploration and quantitative assessment of undiscovered resources.

Acknowledgment

We thank professor Maysam Abedi for his guidance and help in keeping our development on track, and professor Alok Porwal for comments that greatly improved the manuscript.

REFERENCES

[1] E. J. M. Carranza and A. G. Laborte, "Data-driven predictive mapping of gold prospectivity, Baguio district, Philippines: Application of Random Forests algorithm," Ore Geol. Rev., vol. 71, pp. 777–787, 2015.

[2] M. Yousefi and E. J. M. Carranza, "Geometric average of spatial evidence data layers: a GIS-based multi-criteria decision-making approach to mineral prospectivity mapping," Comput. Geosci., vol. 83, pp. 72–79, 2015.

[3] A. Porwal, E. J. M. Carranza, and M. Hale, "Artificial neural networks for

mineral-potential mapping: a case study from Aravalli Province, Western India," Nat. Resour. Res., vol. 12, no. 3, pp. 155–171, 2003.

[4] M. Abedi, G.-H. Norouzi, and N. Fathianpour, "Fuzzy outranking approach: a knowledge-driven method for mineral prospectivity mapping," Int. J. Appl. Earth Obs. Geoinf., vol. 21, pp. 556–567, 2013.

[5] M. Abedi, S. A. Torabi, G.-H. Norouzi, and M. Hamzeh, "ELECTRE III: A knowledge-driven method for integration of geophysical data with geological and geochemical data in mineral prospectivity mapping," J. Appl. Geophys., vol. 87, pp. 9–18, 2012.

[6] M. Abedi, S. B. M. Kashani, G.-H. Norouzi, and M. Yousefi, "A deposit scale mineral prospectivity analysis: A comparison of various knowledge-driven approaches for porphyry copper targeting in Seridune, Iran," J. African Earth Sci., vol. 128, pp. 127–146, 2017.

[7] M. Shabankareh and A. Hezarkhani, "Application of support vector machines for copper potential mapping in Kerman region, Iran," J. African Earth Sci., vol. 128, pp. 116–126, 2017.

[8] S. Ghasemzadeh, A. Maghsoudi, M. Yousefi, and M. J. Mihalasky, "Stream sediment geochemical data analysis for district-scale mineral exploration targeting: Measuring the performance of the spatial U-statistic and CA fractal modeling," Ore Geol. Rev., vol. 113, p. 103115, 2019.

[9] H. Rahimi, M. Abedi, M. Yousefi, A. Bahroudi, and G. R. Elyasi, "Supervised mineral exploration targeting and the challenges with the selection of deposit and non-deposit sites thereof," Appl. Geochemistry, vol. 128, no. December 2020, p. 104940, 2021.

[10] G. F. Bonham-Carter, "Geographic information systems for geoscientists-modeling with GIS," Comput. methods Geosci., vol. 13, p. 398, 1994.

[11] L. Zürcher et al., "Porphyry copper assessment of the Tethys region of western and southern Asia: Chapter V in Global mineral resource assessment," US Geological Survey, 2015.

[12] J. D. Lowell and J. M. Gumbert, "Lateral and vertical alteration-mineralization zoning in porphyry ore deposits: Econ," in Geol, 1970.

[13] R. H. Sillitoe, "Porphyry copper systems," Econ. Geol., vol. 105, no. 1, pp. 3–41, Jan. 2010.

[14] A. P. Crosta, C. R. De Souza Filho, F. Azevedo, and C. Brodie, "Targeting key alteration minerals in epithermal deposits in Patagonia, Argentina, using ASTER imagery and principal component analysis," Int. J. Remote Sens., vol. 24, no. 21, pp. 4233–4240, 2003.

[15] F. A. Kruse et al., "The spectral image processing system (SIPS)—interactive visualization and analysis of imaging spectrometer data," Remote Sens. Environ., vol. 44, no. 2–3, pp. 145–163, 1993.

[16] G. I. Tripp, "Nature of the Archaean zuleika shear zone, Kalgoorlie, Western Australia," in Applied Structural Geology for Mineral Exploration and Mining, Kalgoorlie 2002, Australian Institute of Geoscientists, Extended Abstracts, 2002, pp. 212–215.

[17] G. I. Tripp, "Fault control on Archaean gold deposits, Ora Banda, Western Australia," Aust. Inst. Geosci. Newsl., vol. 62, pp. 1–6, 2000.

[18] R. H. Sibson, "Earthquake rupturing as a mineralizing agent in hydrothermal systems.," Geology, vol. 15, no. 8, pp. 701–704, Aug. 1987.

[19] D. P. Cox, "Descriptive model of porphyry Cu," Miner. Depos. Model. US Geol. Surv. Bull., vol. 1693, p. 76, 1986.

[20] R. M. Tosdal, "Magmatic and structural controls on the development of porphyry Cu±Mo±Au deposits," Rev. Econ. Geol., vol. 14, pp. 157–181, 2001.

[21] H. O. Safari, L. Bagas, and B. Shafiei Bafti, "Structural controls on the localization of Cu deposits in the Kerman Cu metallogenic province of Iran using geoinformatic techniques," Ore Geol. Rev., vol. 67, pp. 43–56, 2015.

[22] E. J. M. Carranza, Geochemical anomaly and mineral prospectivity mapping in GIS, vol. 11. Elsevier, 2008.

[23] A. Porwal, E. J. M. Carranza, and M. Hale, "Knowledge-driven and data-driven fuzzy models for predictive mineral potential mapping," Nat. Resour. Res., vol. 12, no. 1, pp. 1–25, 2003.

[24] A. Porwal, E. J. M. Carranza, and M. Hale, "A hybrid neuro-fuzzy model for mineral potential mapping," Math. Geol., vol. 36, no. 7, pp. 803–826, 2004.

[25] A. Porwal, E. J. M. Carranza, and M. Hale, "A hybrid fuzzy weights-of-evidence model for mineral potential mapping," Nat. Resour. Res., vol. 15, no. 1, pp. 1–14, 2006.

[26] M. Yousefi, A. Kamkar-Rouhani, and E. J. M. Carranza, "Geochemical mineralization probability index (GMPI): a new approach to generate enhanced stream sediment geochemical evidential map for increasing probability of success in mineral potential mapping," J. Geochemical Explor., vol. 115, pp. 24–35, 2012.

[27] M. Yousefi and E. J. M. Carranza, "Fuzzification of continuous-value spatial evidence for mineral prospectivity mapping," Comput. Geosci., vol. 74, pp. 97–109, 2015.

[28] M. Yousefi, E. J. M. Carranza, and A. Kamkar-Rouhani, "Weighted drainage catchment basin mapping of stream sediment geochemical anomalies for mineral potential mapping," J. Geochemical Explor., vol. 128, pp. 88–96, 2013.

[29] M. Yousefi and E. J. M. Carranza, "Data-driven index overlay and Boolean logic mineral prospectivity modeling in greenfields exploration," Nat. Resour. Res., vol. 25, no. 1, pp. 3–18, 2016.

[30] M. J. Mihalasky and G. F. Bonham-Carter, "Lithodiversity and its spatial association with metallic mineral sites, Great Basin of Nevada," Nat. Resour. Res., vol. 10, no. 3, pp. 209–226, 2001.

[31] M. Yousefi and J. M. A. Hronsky, "Translation of the function of hydrothermal mineralization-related focused fluid flux into a mappable exploration criterion for mineral exploration targeting," Appl. Geochemistry, vol. 149, no. January, p. 105561, 2023.

[32] G. Last and M. Holtmann, "1 Introduction 2 Some general facts."

[33] S. J. Yousefia, H. Ranjbar, S. Alirezaeics, S. Dargahid, and D. R. Lentze, "Comparison of Hydrothermal Alteration Patterns Associated with Porphyry Cu Deposits hosted by Granitoids and Intermediate-mafic Volcanic rocks, Kerman Magmatic Arc, Iran: application of geological, mineralogical and remote sensing data," J. African Earth Sci., vol. 142, pp. 112–123, 2018.

[34] M. D. Dimitrijevic and I. Djokovic, Geological Map of Kerman Region. Institute for geological and mining exploration and investigation of nuclear and other mineral raw materials, 1973.We thank professor Maysam Abedi for his guidance and help in keeping our development on track, and professor Alok Porwal for comments that greatly improved the manuscript.